

The Effect of Stellar Velocity on Dark Matter Capture and Detection with Population III Stars

Cosmin Ilie,^{a,b,1} Jillian Paulin^a

^aDepartment of Physics and Astronomy, Colgate University
13 Oak Dr., Hamilton, NY 13346, U.S.A.

^bDepartment of Theoretical Physics, National Institute for Physics and Nuclear Engineering
Magurele, P.O.Box M.G. 6, Romania

E-mail: cilie@colgate.edu, jpaulin@colgate.edu

Abstract. Compact astrophysical objects have been considered in the literature as dark matter (DM) probes, via the observational effects of annihilating captured DM. In this respect, Population III (Pop III) stars are particularly interesting candidates, since they form at high redshifts, in very high DM density environments. It is customary to assume such a star would form roughly at the center of a DM halo, and, as such, have no rotational velocity. In this paper, we break from this assumption and explore the effects we can expect to observe if a Pop III star forms at some distance away from the center of the halo and thus has a non-zero rotational velocity. The capture rate of DM in such a star is suppressed by a predictable amount. We develop— and validate— an analytical expression for the capture rate suppression factor and re-evaluate the bounds placed on the DM-nucleon cross section as a result of DM capture. We find that our previous results, obtained under the assumption of star formed within the central 10 AU of the DM mini-halo are essentially unchanged, even when considering the possible rotational velocities for those central stars.

¹Corresponding author.

Contents

1	Introduction	1
2	DM Capture	2
3	Analytical Evaluation of the Boosted Capture Rate	8
4	Bounds on the DM-Nucleon Cross Section	10
5	Conclusion	11

1 Introduction

Population III (abbreviated Pop III) stars may have been the first stars in the universe, and would have been composed entirely of hydrogen and helium, and powered by nuclear fusion. They formed inside of DM mini-halos with a virial mass $M_{halo} \sim 10^6 M_{\odot}$, at redshifts $z \sim 10 - 40$. Hydrodynamical simulations lead to the following consensus in the literature: typically one or just a few Pop III stars form per mini-halo, within the inner 10 AU of the center, with masses up to $\sim 1000 M_{\odot}$, powered by nuclear hydrogen burning [1, 10, 16, 17, 30, 39, 43, 53, 54]. As the pristine (BBN generated) molecular hydrogen and helium gas cools, it will start following the gravitational potential of the DM wells that began forming the first mini-halos in what is called hierarchical structure formation. During the collapse process, the gas heats up, and various chemical processes become important. The interplay between all heating and all cooling mechanisms available will, ultimately, dictate when the runaway collapse is halted by thermal pressure alone. At this stage a proto-star much less massive than $1 M_{\odot}$ is formed. Over time, as these objects grow in mass through accretion and become hotter and hotter, they begin their lives as stars on the Zero Age Main Sequence (ZAMS), with masses up to $\sim 1000 M_{\odot}$.

DM heating during the formation of the first stars could halt the protostellar gas cloud collapse well before the ignition of nuclear fusion, under conditions first identified by [50]. This would lead to the formation of objects powered mainly by DM annihilations, i.e. Dark Stars (DS). Those hypothetical objects can grow to be supermassive [25] and have different photometric signatures compared to Pop III stars [31, 56]. In this work we assume that at least some of the first stars that will be observed by JWST are Pop III stars, which can be used as DM probes [32, 33, 35].

As with all celestial bodies, these stars (Pop III or Dark Stars) have the potential to capture particles of DM [26, 38]. Understanding how the evolution of Pop III stars is affected by the capture of DM can help us to better understand the properties of DM. In [32, 33] some of the most stringent bounds, to-date, on the spin-dependent (SD) and spin-independent (SI) DM-proton scattering cross sections were placed in Ref. [33] by using the candidate Pop III $z \sim 7$ system identified by Ref. [52] in the HST data.

Today, there are numerous viable theories on the nature of DM. Some of the most notable include: weakly interacting massive particles (WIMPs) [see 48, and references therein], WIMPZILLAs [40], and axions or axion-like particles [see 44, and references therein], to name a few. For a while, massive astrophysical compact halo objects (MACHOs) were also popular

candidates [22], and today a related version of this line of reasoning are Primordial Black Holes (PBHs) as DM candidates [19]. There are two distinct strategies for DM detection. One is direct detection, based on the interactions between DM and baryonic matter and the minute energy transferred to nuclei by collisions with the omnipresent sea of DM particles within our galaxy, through which the Earth and the Sun travel [49, for a recent review see]. Any such DM signal should have a clear annual modulation, as predicted by [21]. Intriguingly, such a signal has been detected by the DAMA experiment starting in 1998 [12], and has persisted for more than two decades with an ever increasing statistical significance [13]. It is striking that none of the other direct detection experiments have identified a signal. Recently, two experiments (ANAIS and COSINE) have been set up with the same detector technology (NaI) as the DAMA experiment, and, while preliminary, there is no indication of a statistically significant annual modulation in their data [2, 3]. Other very sensitive DM direct detection searches include the XENON1T [5–9] experiment in Gran Sasso, Italy, the PICO experiment located at SNOLAB in Canada [4], and PandaX-II in China [51], among others. Despite the fact that these experiments have been running for some time, none of them have yet detected DM directly.

Rather than relying solely on direct detection, one can extract DM parameters for any model based on annihilation signals that could originate from DM dense regions. This, in a nutshell, is the essence of indirect detection techniques. For a review see Ref. [23]. For instance, Refs. [26, 32, 33, 35, 36, 38] discuss the impact of DM on a Pop III star’s luminosity. Most stars shine below the Eddington luminosity— that is, the brightest theoretically possible luminosity that preserves hydrostatic equilibrium. However, a star that has accreted enough DM may shine at the Eddington limit, and, as such, a limit on its mass can be placed if we know the DM-proton interaction cross section. Conversely, if a Pop III star is observed, its mere existence implies an upper bound on the cross section.

Most work on DM capture in Pop III stars assumes, based on the outcome of hydrodynamic simulations, that the star will form at the center of the surrounding DM halo. But this may not be the case every time. We ask, if a star were to form at some distance outside of the halo’s center, how would the capture mechanism be affected? More specifically, what would happen to the capture rate of DM, and what does this mean when trying to constrain DM properties? In Section 2, we outline DM capture rates in depth as well as define the amount by which capture becomes suppressed. In Section 3, we find an analytical expression representative of this suppressed capture rate, and find expressions describing the suppression factor. Finally, in Section 4, we establish bounds on the DM-nucleon cross section, and contrast with those previously obtained, when the Pop III star was assumed to have formed at the center of the DM halo. We emphasise that our formalism is not tied to Pop. III stars, and can be applied to any celestial object capturing DM that is that has a non zero velocity with respect to the rest frame of the DM distribution.

2 DM Capture

In this section we give a brief overview of the formalism necessary to predict the capture rates of DM by astrophysical compact objects, such as stars, planets, etc. In order for a DM particle to be captured by a star, its velocity must fall below the star’s escape velocity. This can occur through collisions with baryonic nuclei in the star. Depending on the mass of the DM particle, this may happen after one [28, 29, 47] or more collisions [11, 15, 20, 34]. Namely, a heavy DM particle would take more collisions to be captured than a light DM particle. Additionally,

the number of collisions that are likely to occur depends on the characteristics of the star; this number is roughly equal to the optical depth of the star, $\tau = n_T \sigma (2R_\star)$, where n_T is the average number density of target particles in the star, σ is the cross section of interaction, and R_\star is the stellar radius. In the case of Pop III stars, which are composed primarily of hydrogen, we assume the atomic nuclei to have the mass of one proton. The probability of capture after N scatters may be represented as follows [15, 34]

$$C_N = \pi R_\star^2 p_N(\tau) \int_0^\infty f(u) \frac{du}{u} w^2 g_N(w), \quad (2.1)$$

where R_\star is the radius of the star, $p_N(\tau)$ is the probability of N collisions occurring, $f(u)$ is the DM velocity distribution, and $g_N(w)$ is the probability that the DM particle's velocity will fall below the escape velocity after N scatters. The quantity $p_N(\tau)$ may be represented as [35]:

$$p_N(\tau) = \frac{2}{\tau^2} \left(N + 1 - \frac{\Gamma(N + 2, \tau)}{N!} \right), \quad (2.2)$$

with $\Gamma(a, b)$ is the upper incomplete gamma function defined as $\Gamma(a, b) = \int_b^\infty t^{a-1} e^{-t} dt$. As found in [15], $g_N(w)$ can be approximated with:

$$g_N(w) = \Theta(v_{esc} (1 - \frac{\beta_+}{2})^{-N/2} - w), \quad (2.3)$$

where $\beta_+ = \frac{4m_\chi m_n}{(m_\chi + m_n)^2}$, with m_χ being the DM particle mass, m_n the mass of the target particle, and v_{esc} is the escape velocity at the surface of the star. Additionally, w represents the velocity of a DM particle and is related to the velocity u by $w^2 = v_{esc}^2 + u^2$. In order to determine the total capture rate, we must sum the values of C_N for every value of N :

$$C_{tot} = \sum_{N=1}^{\infty} C_N. \quad (2.4)$$

This is a complete analytical representation of the total capture rate. However, in order to perform a numerical calculation, it is impossible to sum to infinity. Therefore it is necessary to implement a cutoff condition. We continue summing the series until we reach a desired level of accuracy which we arbitrarily set to 0.1%; that is, until one additional iteration of C_N only changes C_{tot} by 0.1%.

In most cases, a Maxwell-Boltzmann velocity distribution has been applied to calculate DM capture rates of Pop III stars. This is because it is typically assumed that they form at the center of DM halos. As a result, they do not have a velocity relative to the halo. However, in the case of stellar formation off-center from the halo, the star will orbit around the center of mass of the system. Considering that the mass of the halo is much greater than the mass of the star, this orbit will be bound very near the halo's center. It therefore has a relative velocity directly related to the star's distance from the halo's center. We point out that the formalism developed here, and the analytical approximations, are valid for any DM capturing object, such as stars, neutron stars, and brown dwarfs. For non-rogue exoplanets one should include the additional effect of the relative motion between the planet itself and the parent star, which would lead to a periodic modulation of the capture rates.

In order to isolate the effects of the stellar velocity on the capture rate, we first consider the extreme case, where the star forms at the scale radius of the halo. This scenario is

highly unlikely, as Pop III stars form much closer to the center of the DM halo; as such the suppression due to Pop III stars’ stellar velocities is expected to be always less than whatever suppression we will find for this benchmark, overly conservative case. At first pass we assume that the halo follows a Navarro-Frenk-White (NFW) profile [45]:

$$\rho_{halo} = \frac{\rho_0}{\frac{r}{r_s} \left(1 + \frac{r}{r_s}\right)^2}, \quad (2.5)$$

where r is the distance from the center and r_s is the scale radius, and for DM mini-halos in which Pop III stars form, it has a value that ranges between 3 and 300 parsecs. ρ_0 is the central density, defined as:

$$\rho_0 = \frac{200}{3} \frac{c_{vir}^3}{\ln(1 + c_{vir}) - \frac{c_{vir}}{c_{vir}+1}} \rho_c, \quad (2.6)$$

where c_{vir} represents a concentration parameter $c_{vir} = \frac{r_{vir}}{r_s}$ and ranges in value from 1 to 10 [24]. ρ_c is the critical density and depends on the redshift z in accordance with the Friedmann equation.

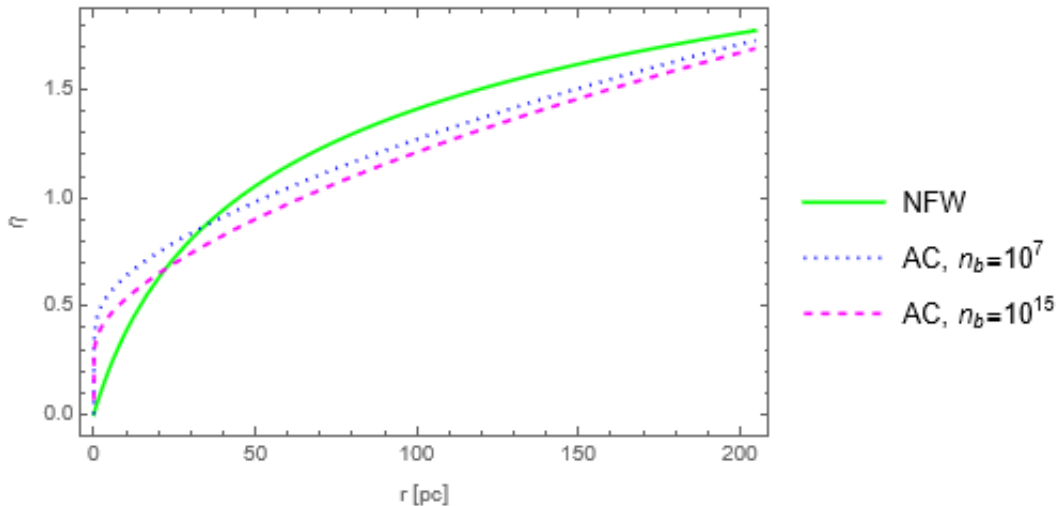


Figure 1. The value of η as a function of the distance from the center of a DM halo under various circumstances; the solid green line represents a standard NFW profile, and both the blue (dotted) and pink (dashed) lines are adiabatically contracted (AC). The blue line takes a core density (n_B) of 10^7cm^{-3} and the pink line takes $n_B = 10^{15} \text{cm}^{-3}$. The total mass of the halo is $10^6 M_\odot$, the redshift is $z = 15$, and the concentration parameter is $c = 10$. Note that as a result of these parameters, the scale radius is 20.47 pc away from the halo’s center. At this location for an NFW profile, $\eta \approx 0.639$; for an AC profile with $n_B = 10^7$, we get $\eta \approx 0.754$; for an AC profile with $n_B = 10^{15}$, we get $\eta \approx 0.655$. An important takeaway is that, within the scale radius—the region with which we are concerned—adiabatic contraction effectively enhances the value of η in comparison to the value expected from a standard NFW profile.

Knowing the density distribution of DM in the halo, we calculate the mass enclosed in the stellar orbit, and thus can easily find the speed at which a Pop III star located at this point would orbit around its center. The stellar velocity will be encoded in a parameter called η , a dimensionless quantity which is defined as:

$$\eta \equiv \sqrt{\frac{3}{2} \frac{\tilde{v}}{\bar{v}}}, \quad (2.7)$$

with \tilde{v} representing the stellar velocity and \bar{v} the dispersion velocity of DM. Adopting the parameters described in the caption to Fig 1, we expect an object located at the scale radius of the halo to have an orbital velocity of $\tilde{v} \approx 5.22 \times 10^5$ cm/s when placed in a standard NFW profile. Of course, changing the redshift or concentration parameter, for instance, would yield slightly different values; we provide an analysis adopting $z = 15$ and $c = 10$ in order to illustrate one example in depth. Including the effects of the adiabatic compression [14, 24, 27, 55] on the DM density profile would not affect much this value, since the mass enclosed within the scale radius will stay roughly constant, as the adiabatic compression operates at smaller, sub-parsec scales. The relation between the value of η and the distance from the halo center is shown in Fig. 1 for a standard NFW profile as well as two adiabatically contracted profiles.

We elaborate below some of the details of the calculation of the dimensionless stellar velocity η . The mass profile of the halo is found by integrating over the density profile considered:

$$M(r) = \int_0^{r_{vir}} \rho_{halo}(r) \times 4\pi r^2 dr, \quad (2.8)$$

where, for an NFW profile, we obtain:

$$M(r) = 4\pi r_s^3 \rho_0 \left[-\frac{r}{(1 + \frac{r}{r_s})r_s} + \ln \left(1 + \frac{r}{r_s} \right) \right]. \quad (2.9)$$

After substituting the mass profile into η , we obtain the following expression for a standard NFW profile:

$$\eta(r) = \frac{\sqrt{\pi}}{50000} \sqrt{\frac{c_{vir}^3 G \rho_c r_s^3 \left(\ln \left(\frac{r}{r_s} + 1 \right) - \frac{r}{r_s \left(\frac{r}{r_s} + 1 \right)} \right)}{r \left(\ln(c_{vir} + 1) - \frac{c_{vir}}{c_{vir} + 1} \right)}}. \quad (2.10)$$

It is now important to consider the DM velocity distribution. Because we assume the star to have a velocity relative to the halo, we need to apply a boosted velocity distribution rather than the traditional Maxwell-Boltzmann distribution. The boosted distribution f_η is directly related to the Maxwell-Boltzmann distribution f_0 [29]:

$$f_0(u) du = n_\chi \frac{4}{\sqrt{\pi}} x^2 \exp(-x^2) dx, \quad (2.11)$$

where n_χ is the number density of DM particles, x is a dimensionless quantity defined as $x \equiv \frac{m_\chi}{2kT_W} u^2$, with k as the Boltzmann constant and T_W as the DM temperature, representing the velocity of the DM particles normalized to their thermal average value. The boosted distribution is then defined as in [29]:

$$f_\eta(u) = f_0(u) \exp(-\eta^2) \frac{\sinh(2x\eta)}{2x\eta} \quad (2.12)$$

Therefore, for a Pop III star located at the scale radius of a DM halo, if we take $\bar{v} = 10^6$ cm/s (which is a typical value for DM mini-halos hosting Pop III stars; as in [35], \bar{v} ranges from $10^5 - 1.5 \times 10^6$ cm/s.) and $\tilde{v} = 5.22 \times 10^5$ cm/s as calculated above, then the value of η

is ≈ 0.639 . This is a reasonable maximum bound to use when considering boosted capture of Pop III stars, because in practice, these stars are expected to form well inside the scale radius of DM halos. In turn, this will lead to the highest possible suppression on the previously calculated capture rates in [32, 33, 35]. Note that in our capture rate calculation, since we are mainly focusing on the effect of stellar velocity, we take the assumption that the DM density is fixed, i.e. is the same value at the scale radius as at the halo center.

In order to numerically calculate the capture rate of DM, we need to adopt parameters of Pop III stars from numerical simulations. Although Pop III stars are still theoretical objects and have not been observed, simulations have been done, allowing one to test several valid combinations of mass, radius and luminosity [37, 46]. In [35], it has been shown that Pop III stars have two different homology scaling relations (in two different mass regimes), where stars with a mass $M_\star < 20M_\odot$ follow $R_\star \propto M_\star^{0.21}$, and larger mass stars follow $R_\star \propto M_\star^{0.56}$.

Since our aim in this paper is to understand and quantify the effects of the stellar velocity on DM capture, we assume, for now, the same ambient density at the location of the star, in order to disambiguate between the suppression due to an increase in the stellar velocity, and the decrease in the DM density. Both of those lead to a suppression in the capture rate. For the latter, the effect is trivial, since the total capture rate scales linearly with the DM density: $C_{tot} \sim \rho_\chi$. Our aim is to obtain a simple, analytic procedure, that would estimate the suppression rate on capture rates by any astrophysical object, if the parameter η is known. Previous work in the literature that use compact astrophysical objects as DM probes, typically neglect the effects of the stellar velocity. For example Neutron Stars are considered by [15], and exoplanets by [41], and both works neglect the possible role of the relative velocity between the capturing object and the DM halo. The formalism we will develop in Section 3 can be easily applied to any such scenario, if the location (and therefore velocity) of the object in question is known.

In Fig 2 we contrast the total capture rates of DM by an arbitrary Pop III star, first placed at the center of the DM halo (as previously assumed) and then placed at the scale radius of the DM halo. We note that, to a good approximation, the capture rates remain unaffected by the inclusion of the stellar velocity, for the case of Pop III stars. When the boosted distribution is applied, the DM capture rate (see Eq 2.1) is suppressed, as one may expect. We next take the ratio between the capture rates calculated using a boosted ($\eta \neq 0$) and a regular ($\eta = 0$) Maxwell-Boltzmann distribution to illustrate the amount by which capture is suppressed. As shown in Figure 3, the ratio plateaus for low and high DM masses. Notice that the drastic change in this ratio occurs when the DM mass reaches 10^5 GeV, which corresponds exactly to the m_χ for which the quantity $k = 3 \frac{m}{m_\chi} \frac{v_{esc}^2}{v^2}$, defined in [32], reaches a value of 1.

In the next section we present an analytical approximation of the suppression factor for the DM capture rates, in both the low (i.e. $k \gg 1$) and high (i.e. $k \ll 1$) DM mass regimes. This can be very useful when one needs to estimate the effects of the stellar velocity on DM capture rates, and implicitly on DM scattering cross section bounds, since calculating numerically the capture rates including the full, boosted MB distribution can be quite computationally expensive. Our procedure allows one to calculate the simpler, and fully analytically solvable [32] rates when the stellar velocity is neglected, and then apply the suppression factor we derive for any given η . Such a procedure is quite useful when considering capture of DM by astrophysical probes within the Solar System neighborhood, where, based on DM profile [42] and dispersion velocity [18] estimates, we would expect η to be on the order of a few.

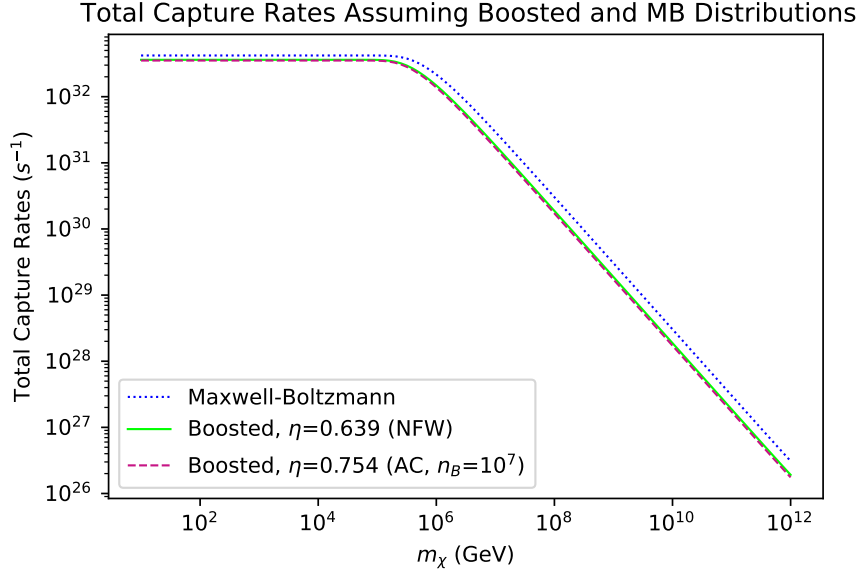


Figure 2. DM capture rates for a $1000 M_{\odot}$ Pop III star, assuming $\rho_{\chi} = 10^9 \text{ GeV}/\text{cm}^3$. The (dotted) blue line shows the total capture rate when assuming a Maxwell-Boltzmann velocity distribution, and the (solid) green and (dashed) pink lines assume a boosted distribution. The green line assumes an NFW profile whereas the pink line is adiabatically contracted with a central density of 10^7 . Although the capture rates look very close on this graph, the boosted capture rate is actually suppressed by a significant factor. Refer to Figure 3 for a more thorough understanding of the value of this factor.

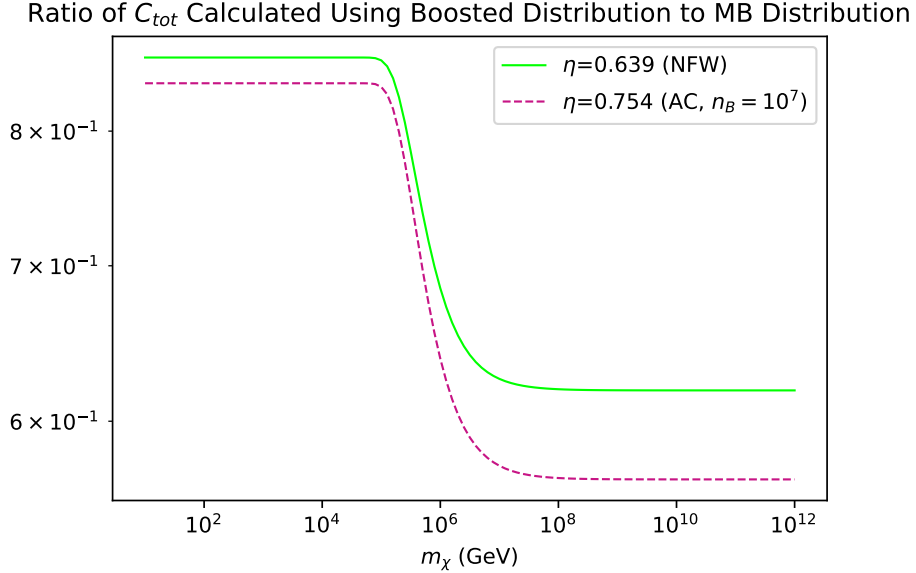


Figure 3. The ratio of the total capture rates of the same Pop III star as in Fig 2. The solid green line represents an NFW profile and the dashed pink line represents an adiabatically contracted profile. The low mass regime is suppressed by a smaller factor than the high mass regime, although both plateau with a transition in trends near $m_{\chi} = 10^6$ GeV.

3 Analytical Evaluation of the Boosted Capture Rate

Rather than integrating over the DM velocity distribution numerically to calculate a boosted capture rate, we can find an equivalent analytical expression. In order to develop this, we followed a similar method to [15, 34]. The main difference comes from the use of the boosted velocity distribution as outlined by [29] instead of the assumption of a Maxwell-Boltzmann distribution. Evaluating 2.1 by replacing $f(u)$ with 2.12, we obtain:

$$\begin{aligned}
C_N = & \frac{n_\chi \pi p_N(\tau) R^2}{2\sqrt{6}\bar{v}\eta} \left[\frac{1}{\sqrt{\pi}} \exp\left(\frac{-3(v_N^2 - v_{esc}^2)}{\bar{v}^2} - 2\eta^2\right) \bar{v} \left\{ 4 \exp\left(\frac{3(v_N^2 - v_{esc}^2)}{\bar{v}^2} + \eta^2\right) \bar{v}\eta + \right. \right. \\
& \exp\left(\frac{-6v_{esc}^2 + 6v_N^2 - 4\sqrt{6}v_{esc}\bar{v}\eta\sqrt{-1 + \frac{v_N^2}{v_{esc}^2} + 4\bar{v}^2\eta^2}}{4\bar{v}^2}\right) \left(\sqrt{6}v_{esc}\sqrt{-1 + \frac{v_N^2}{v_{esc}^2}} - 2\bar{v}\eta\right) - \\
& \exp\left(\left(\frac{\sqrt{\frac{3}{2}}v_{esc}\sqrt{-1 + \frac{v_N^2}{v_{esc}^2}}}{\bar{v}} + \eta\right)^2\right) \left(\sqrt{6}v_{esc}\sqrt{-1 + \frac{v_N^2}{v_{esc}^2}} + 2\bar{v}\eta\right) \left. \right\} + \\
& (3v_{esc}^2 + \bar{v}^2(1 + 2\eta^2)) \operatorname{erf}\left(\frac{\sqrt{\frac{3}{2}}v_{esc}\sqrt{-1 + \frac{v_N^2}{v_{esc}^2}}}{\bar{v}} - \eta\right) + \\
& 2(3v_{esc}^2 + \bar{v}^2(1 + 2\eta^2)) \operatorname{erf}(\eta) - \\
& \left. (3v_{esc}^2 + \bar{v}^2(1 + 2\eta^2)) \operatorname{erf}\left(\frac{\sqrt{\frac{3}{2}}v_{esc}\sqrt{-1 + \frac{v_N^2}{v_{esc}^2}}}{\bar{v}} + \eta\right) \right], \quad (3.1)
\end{aligned}$$

where the quantity v_N is defined as follows:

$$v_N = v_{esc} \left(1 - \frac{\beta_+}{2}\right)^{\frac{-N}{2}}. \quad (3.2)$$

As a sanity check, we verify that in the limit of $\eta = 0$, the expression reduces to that in [15, 34]:

$$\lim_{\eta \rightarrow 0} C_N = \sqrt{\frac{2\pi}{3}} \frac{n_\chi p_N(\tau) R^2}{\bar{v}} \left[(2\bar{v}^2 + 3v_{esc}^2) - \exp\left(\frac{-3(v_N^2 - v_{esc}^2)}{2\bar{v}^2}\right) (3v_N^2 + 2\bar{v}^2) \right]. \quad (3.3)$$

The expression of C_N presented in Eq.(3.1) is not particularly illuminating. However, we can use it to analytically evaluate the suppression factor due to the boosted distribution. The fit for the ratio must be divided into two regimes, one for low DM mass and one for high DM mass. A way to distinguish whether DM mass is high or low is to look for when the quantity $k = 3\frac{m}{m_\chi} \frac{v_{esc}^2}{\bar{v}^2}$ crosses 1; when k is large, then m_χ is small and vice versa. In either case, the suppression factor is obtained by dividing the integral over the boosted distribution

$f_\eta(u)$ (Eq 2.12) by the integral over the Maxwell-Boltzmann distribution $f_0(u)$ (Eq 2.11), and expanding around x_{max} , the upper bound of integration (that is, the dimensionless maximum capture speed of DM particles, where $x_{max} = \sqrt{\frac{3}{2}} \frac{u_{max}}{\bar{v}}$, and where u_{max} is based on Eq 2.3, with $u_{max} = v_{esc}((1 - \frac{\beta_\pm}{2})^{-N} - 1)^{\frac{1}{2}}$):

$$\text{Suppression Factor} = \frac{\int_0^{x_{max}} f_\eta dx}{\int_0^{x_{max}} f_0 dx}. \quad (3.4)$$

We expand the suppression factor, as defined above, around $x_{max} \rightarrow 0$ in the high mass regime, and around $x_{max} \rightarrow \infty$ in the low-mass regime. Therefore, the suppression factor in the low mass regime may be evaluated with the following approximation:

$$\text{Ratio}_{\text{low } m_\chi} = \frac{e^{-\eta^2} \left(4\eta + \frac{6e\eta^2 \sqrt{\pi} v_{esc}^2 \text{erf}(\eta)}{\bar{v}^2} + 2e\eta^2 \sqrt{\pi} (1 + 2\eta^2) \text{erf}(\eta) \right)}{4 \left(2 + \frac{3v_{esc}^2}{\bar{v}^2} \right) \eta}. \quad (3.5)$$

For the high-mass regime, it is approximated by:

$$\text{Ratio}_{\text{high } m_\chi} = e^{-\eta^2} + \frac{1}{3} e^{-\eta^2} \eta^2 x_{max}^2 + \frac{e^{-\eta^2} \eta^2 (10\bar{v} - 15v_{esc}^2 + 12v_{esc}^2 \eta^2) x_{max}^4}{270v_{esc}^2}. \quad (3.6)$$

These fits, along with the numerically-calculated ratio (as in Fig 3) are shown in Fig 4.

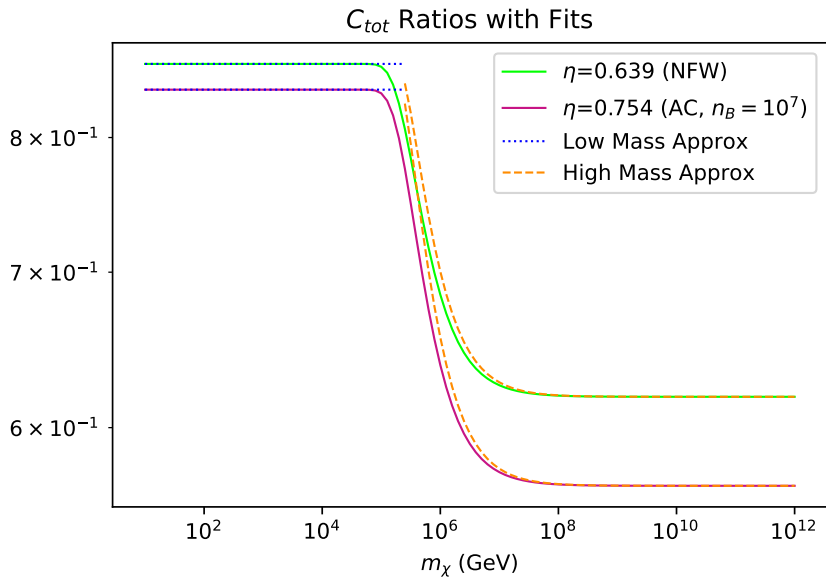


Figure 4. The numerically-calculated suppression factor for the DM capture rate of a Pop III star is shown in green for an NFW halo, and in pink for an AC halo (as in Fig 3). The blue (dotted) lines show the fit for the low-mass regime. The orange (dashed) lines approximate the high-mass regime. Note the excellent agreement between the numerical results (green and pink) and our analytic approximations, on their respective domains.

In summary, we have presented and validated simple analytical formulae for the suppression factors of the capture rates in terms of the dimensionless stellar velocity $\eta \equiv \sqrt{\frac{3}{2}} \frac{\bar{v}}{v}$. For

any given DM mass one can evaluate the value of $k \equiv \frac{3m}{m_\chi} \frac{v_{esc}^2}{v^2}$. If $k \gg 1$, i.e. for “low” m_χ then the suppression factor is given by Eq 3.5, whereas for $k \ll 1$, i.e. “high” m_χ the suppression can be estimated by using Eq 3.6. In the next section we include the effects of the suppression of the capture rates by stellar velocities when obtaining DM-proton cross section upper bounds by using Pop III stars as probes.

4 Bounds on the DM-Nucleon Cross Section

In the previous section, we found a fit to match the suppression in capture rate due to the relative velocity between a star and the DM halo. Here, we further validate this fit, and show it’s usefulness, by revisiting the bounds on the cross section of interaction between DM and atomic nuclei when Pop III stars are used as DM probes, and when the possible effects of the stellar rotational velocity are included.

Prior works such as [32, 33] constrain the bounds on the cross section of interaction between DM and baryonic particles due to the impact DM has on the luminosity of Pop III stars. Any object that is gravitationally bound, such as a star, will have an upper bound on how bright it can shine, at a given mass, i.e. the Eddington limit:

$$L_{Edd} \leq L_{nuc} + L_{DM}, \quad (4.1)$$

where L_{nuc} is the luminosity due to nuclear fusion, and L_{DM} is the additional luminosity provided by DM annihilations, which is directly related to the amount of DM captured:

$$L_{DM} = f C_{tot} m_\chi, \quad (4.2)$$

where f is the efficiency with which DM annihilation contributes to the luminosity of the star, i.e. the amount of energy thermalized with the star. The remainder $1 - f$ is lost to products of annihilation that escape, such as neutrinos. Because C_{tot} is dependent on σ , we can numerically calculate the maximum expected value of the cross section by finding the maximum value of L_{DM} . Recall that the Eddington luminosity is given by

$$L_{Edd} = \frac{4\pi c G M_\star}{\kappa_\rho}, \quad (4.3)$$

where c is the speed of light, G is the gravitational constant, M_\star is the stellar mass, and κ_ρ is the opacity of the stellar atmosphere.

The value of L_{nuc} is dependent on the mass of the star, and here we use the fitting form found in [32], which we reproduce here for convenience:

$$L_{nuc} \simeq 10^{\frac{\log(3.71 \times 10^4 L_\odot \text{s/erg})}{1 + \exp(-0.85 \log(x) - 1.95)}} \cdot x^{\frac{2.01}{0.48 + 1}} \text{ erg /s}. \quad (4.4)$$

Since capture rate is suppressed, when including the effects of the stellar velocity, the bounds shift upwards and become less stringent, as illustrated in Figure 5. However, note that the values of $\eta = 0.693$ and $\eta = 0.754$ considered here, are for Pop III stars, unrealistically high. That is because they correspond to the star at the scale radius of the DM halo, which is many orders of magnitude above the typically expected maximum tens of AU from the center where Pop III stars form. Even with this exaggerated value we note that the suppression in the capture rates, and correspondingly the weakening of the cross section bounds are, at most approximately 40%. This suppression has a negligible effect on constraints placed on the DM-nucleon cross section, as demonstrated in Fig 5.

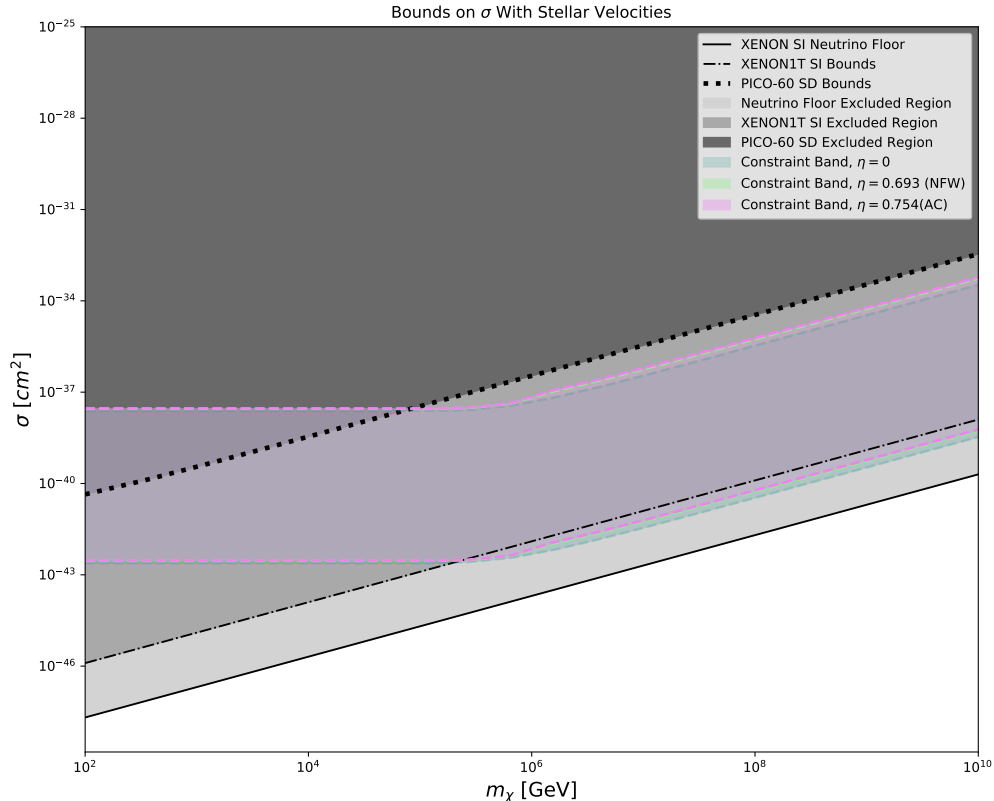


Figure 5. Bounds on the cross section for $\eta = 0$ (blue), $\eta = 0.693$ (green), and $\eta = 0.754$ (pink) for a $1000 M_{\odot}$ Pop III star. The bands represent DM densities ranging from 10^9 GeV cm^{-3} (upper bounds) to $10^{14} \text{ GeV cm}^{-3}$ (lower bounds). There is no significant difference in the bounds on the cross section for all of the values of eta tested. The slight difference between these three scenarios comes from a factor of the inverse of the suppression factor described in Section 3.

5 Conclusion

In this paper we presented and validated an analytic approximation of the suppression factor for the capture rates of DM by astrophysical objects that have a non zero velocity with respect to the DM halo: equations 3.5 and 3.6. When applied to Pop III stars, we find that the role of the stellar velocity can be safely neglected, and all of our previous results, where we considered Pop III stars at the center at the mini-halo, i.e. with zero velocity, remain largely unchanged. This is because the DM capture rate is suppressed by a factor of 57% at the most, for high mass DM particles, and when the star is considered to have formed— or migrated— all the way to the scale radius of the DM halo, which is a highly unrealistic scenario. In most cases Pop III stars will live much closer to the center of the DM halo, within the inner 10 AU or so. Our formalism is even more relevant for astrophysical objects within the Milky Way that act as DM probes, such as neutron stars, brown dwarfs, exoplanets. In this case, the most promising location, the center of the Milky Way, is the site of a supermassive black hole,

which would lead to very large rotational velocities, when compared to the center of high redshift DM microhalos, and therefore larger suppression factors for the DM capture. In a separate publication we plan to investigate this aspect in more detail.

Acknowledgments

JP thanks the financial support from Colgate University, via the Research Council student wage grant, and the Justus '43 and Jayne Schlichting Student Research Funds.

References

- [1] Tom Abel, Greg L. Bryan, and Michael L. Norman. The formation of the first star in the Universe. *Science*, 295:93, 2002.
- [2] G. Adhikari, P. Adhikari, E. Barbosa de Souza, N. Carlin, S. Choi, M. Djamel, A. C. Ezeribe, C. Ha, I. S. Hahn, E. J. Jeon, J. H. Jo, H. W. Joo, W. G. Kang, W. Kang, M. Kauer, G. S. Kim, H. Kim, H. J. Kim, K. W. Kim, N. Y. Kim, S. K. Kim, Y. D. Kim, Y. H. Kim, Y. J. Ko, V. A. Kudryavtsev, H. S. Lee, J. Lee, J. Y. Lee, M. H. Lee, D. S. Leonard, W. A. Lynch, R. H. Maruyama, F. Mouton, S. L. Olsen, B. J. Park, H. K. Park, H. S. Park, K. S. Park, R. L. C. Pitta, H. Prihtiadi, S. J. Ra, C. Rott, K. A. Shin, A. Scarff, N. J. C. Spooner, W. G. Thompson, L. Yang, and G. H. Yu. Search for a dark matter-induced annual modulation signal in nai(tl) with the cosine-100 experiment. *Phys. Rev. Lett.*, 123:031302, Jul 2019.
- [3] J. Amare et al. Annual Modulation Results from Three Years Exposure of ANAIS-112. *Phys. Rev. D*, 103(10):102005, 2021.
- [4] C. Amole et al. Dark Matter Search Results from the Complete Exposure of the PICO-60 C₃F₈ Bubble Chamber. *Phys. Rev. D*, 100(2):022001, 2019.
- [5] E. Aprile, M. Alfonsi, K. Arisaka, F. Arneodo, C. Balan, L. Baudis, B. Bauermeister, A. Behrens, P. Beltrame, K. Bokeloh, and et al. Dark matter results from 225 live days of xenon100 data. *Physical Review Letters*, 109(18), Nov 2012.
- [6] E. Aprile and et al. Dark matter search results from a one ton-year exposure of xenon1t. *Phys. Rev. Lett.*, 121:111302, Sep 2018.
- [7] E. Aprile and et al. Constraining the spin-dependent wimp-nucleon cross sections with xenon1t. *Phys. Rev. Lett.*, 122:141301, Apr 2019.
- [8] E. Aprile et al. Search for Light Dark Matter Interactions Enhanced by the Migdal Effect or Bremsstrahlung in XENON1T. *Phys. Rev. Lett.*, 123(24):241803, 2019.
- [9] E. Aprile et al. Observation of Excess Electronic Recoil Events in XENON1T. *arXiv e-prints*, 6 2020.
- [10] Rennan Barkana and Abraham Loeb. In the beginning: The First sources of light and the reionization of the Universe. *Phys. Rept.*, 349:125–238, 2001.
- [11] Nicole F. Bell, Giorgio Busoni, Sandra Robles, and Michael Virgato. Improved Treatment of Dark Matter Capture in Neutron Stars. *arXiv e-prints*, page arXiv:2004.14888, April 2020.
- [12] R Bernabei, P Belli, F Montecchia, W Di Nicolantonio, A Incicchitti, D Prosperi, C Bacci, C.J Dai, L.K Ding, H.H Kuang, and J.M Ma. Searching for wimps by the annual modulation signature. *Physics Letters B*, 424(1):195 – 201, 1998.
- [13] R. Bernabei et al. First model independent results from DAMA/LIBRA-phase2. *Nucl. Phys. Atom. Energy*, 19(4):307–325, 2018.
- [14] George R. Blumenthal, S. M. Faber, Ricardo Flores, and Joel R. Primack. Contraction of Dark Matter Galactic Halos Due to Baryonic Infall. *Astrophys. J.*, 301:27, 1986.

- [15] Joseph Bramante, Antonio Delgado, and Adam Martin. Multiscatter stellar capture of dark matter. *Phys. Rev. D*, 96(6):063002, Sep 2017.
- [16] Volker Bromm. Formation of the First Stars. *Rept. Prog. Phys.*, 76:112901, 2013.
- [17] Volker Bromm and Richard B. Larson. The First stars. *Ann. Rev. Astron. Astrophys.*, 42:79–118, 2004.
- [18] Warren R. Brown, Margaret J. Geller, Scott J. Kenyon, and Antonaldo Diaferio. Velocity dispersion profile of the milky way halo. *The Astronomical Journal*, 139(1):59–67, Nov 2009.
- [19] Bernard Carr and Florian Kuhnel. Primordial Black Holes as Dark Matter: Recent Developments. *Ann. Rev. Nucl. Part. Sci.*, 70:355–394, 2020.
- [20] Basudeb Dasgupta, Aritra Gupta, and Anupam Ray. Dark matter capture in celestial objects: Improved treatment of multiple scattering and updated constraints from white dwarfs. *JCAP*, 08:018, 2019.
- [21] Andrzej K. Drukier, Katherine Freese, and David N. Spergel. Detecting cold dark-matter candidates. *Phys. Rev. D*, 33:3495–3508, Jun 1986.
- [22] N. W. Evans and V. Belokurov. RIP: The MACHO Era (1974-2004). In *5th International Workshop on the Identification of Dark Matter*, 11 2004.
- [23] Jonathan L. Feng, Konstantin T. Matchev, and Frank Wilczek. Prospects for indirect detection of neutralino dark matter. *Phys. Rev. D*, 63:045024, 2001.
- [24] Katherine Freese, Paolo Gondolo, J.A. Sellwood, and Douglas Spolyar. Dark Matter Densities during the Formation of the First Stars and in Dark Stars. *Astrophys. J.*, 693:1563–1569, 2009.
- [25] Katherine Freese, Cosmin Ilie, Douglas Spolyar, Monica Valluri, and Peter Bodenheimer. Supermassive Dark Stars: Detectable in JWST. *Astrophys. J.*, 716:1397–1407, 2010.
- [26] Katherine Freese, Douglas Spolyar, and Anthony Aguirre. Dark Matter Capture in the first star: a Power source and a limit on Stellar Mass. *JCAP*, 0811:014, 2008.
- [27] Oleg Y. Gnedin, Daniel Ceverino, Nickolay Y. Gnedin, Anatoly A. Klypin, Andrey V. Kravtsov, Robyn Levine, Daisuke Nagai, and Gustavo Yepes. Halo Contraction Effect in Hydrodynamic Simulations of Galaxy Formation. *arXiv e-prints*, page arXiv:1108.5736, August 2011.
- [28] A. Gould. Resonant enhancements in weakly interacting massive particle capture by the earth. *ApJ*, 321:571–585, October 1987.
- [29] Andrew Gould. Direct and Indirect Capture of Wimps by the Earth. *Astrophys. J.*, 328:919–939, 1988.
- [30] Thomas H. Greif, Volker Bromm, Paul C. Clark, Simon C. O. Glover, Rowan J. Smith, Ralf S. Klessen, Naoki Yoshida, and Volker Springel. Formation and evolution of primordial protostellar systems. In Masayuki Umemura and Kazuyuki Omukai, editors, *First Stars IV - from Hayashi to the Future -*, volume 1480 of *American Institute of Physics Conference Series*, pages 51–56, September 2012.
- [31] Cosmin Ilie, Katherine Freese, Monica Valluri, Ilian T. Iliev, and Paul R. Shapiro. Observing supermassive dark stars with James Webb Space Telescope. *MNRAS*, 422(3):2164–2186, May 2012.
- [32] Cosmin Ilie, Caleb Levy, Jacob Pilawa, and Saiyang Zhang. Constraining Dark Matter properties with the first generation of stars. *Phys. Rev. D* (*submitted*), 9 2020.
- [33] Cosmin Ilie, Caleb Levy, Jacob Pilawa, and Saiyang Zhang. Probing below the neutrino floor with the first generation of stars. 9 2020.
- [34] Cosmin Ilie, Jacob Pilawa, and Saiyang Zhang. Comment on “multiscatter stellar capture of dark matter”. *Phys. Rev. D*, 102:048301, Aug 2020.

- [35] Cosmin Ilie and Saiyang Zhang. Multiscatter capture of superheavy dark matter by Pop. III stars. *JCAP*, 12:051, 2019.
- [36] Cosmin Ilie and Saiyang Zhang. Erratum:Multiscatter capture of superheavy dark matter by Pop. III stars (unpublished). *JCAP*, 2020.
- [37] F. Iocco, A. Bressan, E. Ripamonti, R. Schneider, A. Ferrara, and P. Marigo. Dark matter annihilation effects on the first stars. *MNRAS*, 390(4):1655–1669, Nov 2008.
- [38] Fabio Iocco. Dark Matter Capture and Annihilation on the First Stars: Preliminary Estimates. *Astrophys. J.*, 677:L1–L4, 2008.
- [39] Ralf S. Klessen. Formation of the first stars. *arXiv e-prints*, page arXiv:1807.06248, Jul 2018.
- [40] E. W. Kolb, D. J. H. Chung, and A. Riotto. WIMPZILLAS! In H. V. Klapdor-Kleingrothaus and L. Baudis, editors, *Dark matter in Astrophysics and Particle Physics*, page 592, Jan 1999.
- [41] Rebecca K. Leane and Juri Smirnov. Exoplanets as sub-gev dark matter detectors. *Phys. Rev. Lett.*, 126:161101, Apr 2021.
- [42] Hai-Nan Lin and Xin Li. The dark matter profiles in the milky way. *Monthly Notices of the Royal Astronomical Society*, 487(4):5679–5684, Jun 2019.
- [43] Abraham Loeb. *How did the first stars and galaxies form?* Princeton University Press, Princeton, NJ, 2010.
- [44] David J. E. Marsh. Axion Cosmology. *Phys. Rept.*, 643:1–79, 2016.
- [45] Julio F. Navarro, Carlos S. Frenk, and Simon D. M. White. A Universal Density Profile from Hierarchical Clustering. *ApJ*, 490(2):493–508, Dec 1997.
- [46] Takuya Ohkubo, Ken’ichi Nomoto, Hideyuki Umeda, Naoki Yoshida, and Sachiko Tsuruta. Evolution of Very Massive Population III Stars with Mass Accretion from Pre-main Sequence to Collapse. *ApJ*, 706(2):1184–1193, Dec 2009.
- [47] William H. Press and David N. Spergel. Capture by the sun of a galactic population of weakly interacting massive particles. *Astrophys. J.*, 296:679–684, 1985. [,277(1985)].
- [48] Leszek Roszkowski, Enrico Maria Sessolo, and Sebastian Trojanowski. WIMP dark matter candidates and searches—current status and future prospects. *Rept. Prog. Phys.*, 81(6):066201, 2018.
- [49] Marc Schumann. Direct Detection of WIMP Dark Matter: Concepts and Status. *J. Phys. G*, 46(10):103003, 2019.
- [50] Douglas Spolyar, Katherine Freese, and Paolo Gondolo. Dark matter and the first stars: a new phase of stellar evolution. *Phys. Rev. Lett.*, 100:051101, 2008.
- [51] Andi Tan, Mengjiao Xiao, Xiangyi Cui, Xun Chen, Yunhua Chen, Deqing Fang, Changbo Fu, Karl Giboni, Franco Giuliani, Haowei Gong, and et al. Dark matter results from first 98.7 days of data from the pandax-ii experiment. *Physical Review Letters*, 117(12), Sep 2016.
- [52] E. Vanzella, M. Meneghetti, G. B. Caminha, M. Castellano, F. Calura, P. Rosati, C. Grillo, M. Dijkstra, M. Gronke, E. Sani, A. Mercurio, P. Tozzi, M. Nonino, S. Cristiani, M. Mignoli, L. Pentericci, R. Gilli, T. Treu, K. Caputi, G. Cupani, A. Fontana, A. Grazian, and I. Balestra. Candidate Population III stellar complex at $z = 6.629$ in the MUSE Deep Lensed Field. *MNRAS*, 494(1):L81–L85, March 2020.
- [53] Naoki Yoshida, Kazuyuki Omukai, and Lars Hernquist. Protostar Formation in the Early Universe. *Science*, 321:669, 2008.
- [54] Naoki Yoshida, Kazuyuki Omukai, Lars Hernquist, and Tom Abel. Formation of Primordial Stars in a lambda-CDM Universe. *Astrophys. J.*, 652:6–25, 2006.

- [55] P. Young. Numerical models of star clusters with a central black hole. I - Adiabatic models. *ApJ*, 242:1232–1237, December 1980.
- [56] Erik Zackrisson. The observational signatures of high-redshift dark stars. *PoS*, IDM2010:085, 2011.